phys. stat. sol. (b) 85, 715 (1978)

Subject classification: 13 and 20; 22

Department of Physics, The University of British Columbia, Vancouver[1])

Theory of the X-Ray and Optical Properties of Polysulphur Nitride[2])

By

W. I. FRIESEN, D. B. LITVIN, and B. BERGERSEN

The extended Hückel method is used to calculate various band structure dependent properties of polysulphur nitride $(SN)_x$. X-ray emission spectra are computed and are presented as a means of differentiating between conflicting reported band structures. The interband contribution to the imaginary part of the dielectric function is also calculated and is discussed in relation to experimental results quoted in the literature.

Die erweiterte Hückel-Methode wird verwendet, um verschiedene Bandstruktureigenschaften von Poly-Schwefelnitrid $(SN)_x$ zu berechnen. Röntgenemissionsspektren werden berechnet und werden als ein Mittel angegeben, zwischen abweichenden Bandstrukturen zu unterscheiden. Der Beitrag der Interbandübergänge zum Imaginärteil der dielektrischen Funktion wird ebenfalls berechnet und wird in bezug auf veröffentlichte experimentelle Ergebnisse diskutiert.

1. Introduction

The inorganic polymer polysulphur nitride, $(SN)_x$, has several interesting and unusual properties (for a recent review see Greene and Street [1]). The band structure plays an important role in understanding the properties of the material and a large number of calculations have appeared in the last two years. These computations were performed for both a one-dimensional polymeric chain [2 to 7] and for the full three-dimensional crystal structure [8 to 13]. It was found that the interchain interactions, which are responsible for the three-dimensional effects, are crucial for an understanding of properties related to the Fermi surface. Still, the interchain coupling is much weaker than the intrachain interactions, and many of the gross features of the band structure can be determined from calculations for a single chain. All band structures reported so far have been for the monoclinic β-phase. The crystal structure of this phase has been determined by Boudeulle [14, 15], Mikulski et al. [16], and Cohen et al. [17]. According to both structure determinations the atoms constituting a single chain are nearly co-planar with the planes oriented in the (1, 0, 2) direction.

The near planarity of the chains has led several authors to describe the symmetry of their calculated bands as either σ or π, according to whether the wave functions are predominantly symmetric or antisymmetric under reflection through the mean plane of the chain. Utilizing this classification into σ- and π-bands one can separate the published band structures into two categories. In the first category the Fermi energy one lies near the zone boundary at the intersection of two π-bands while in the second the Fermi level intersects two overlapping σ- and π-bands. The two types of results give rise to striking differences in the Fermi surfaces and the density of states.

One way of experimentally distinguishing between the two types of band structures which suggests itself is the measurement of polarized soft X-ray emission spectra.

[1]) Vancouver, British Columbia, Canada, V6T 1W5.

[2]) Research supported by the National Research Council of Canada.

Berg et al. [18] have developed a method of separating the σ- and π-contributions to the valence band in graphite from a determination of the polarization dependence of the K X-ray spectrum. It would probably be difficult to apply this method to the ($\bar{1}02$) plane in $(SN)_x$ because of the problem of twinning; however, oriented films in which this plane is parallel to the substrate have been prepared. Useful information could also be obtained by studying spectra corresponding to polarization parallel or perpendicular to the chain axis and comparing K and $L_{II,III}$ spectra as well as spectra arising from nitrogen or sulphur transitions.

The most striking differences between different band structure calculations are related to the conduction band itself. It is therefore of interest to study theoretically the interband transitions within the conduction band and their polarization dependence (these transitions are mostly in the near-infrared part of the spectrum). Experimental results in this energy range have been reported by Grant et al. [19, 20], Geserich et al. [21], Bright et al. [22], and Bordas et al. [23].

The purpose of the present paper is to report theoretical calculations of the X-ray and near-infra-red spectra of $(SN)_x$ including their polarization dependence. The calculations are based on a slightly modified version of the band structure reported in [8]. The results in the X-ray region are presented in Section 2 while optical spectra are discussed in Section 3. A summary is given in Section 4.

2. X-Ray Emission

In order to derive an expression for the emitted X-ray intensity as a function of energy and polarization we introduce atomic core orbitals $\varphi_{cn}(\boldsymbol{r} - \boldsymbol{r}_n - \boldsymbol{R}_l)$, atomic valence orbitals $\varphi_{vn}(\boldsymbol{r} - \boldsymbol{r}_n - \boldsymbol{R}_l)$ and valence band states $\psi_{\alpha\boldsymbol{k}}(\boldsymbol{r})$. Here $\boldsymbol{R}_l$ is the position vector to the center of the l-th unit cell, $\boldsymbol{r}_n$ is the position vector within the cell of the n-th atom, and α is the band index. The intensity for electronic transitions from an occupied valence band α to an unoccupied core state can be written

$$I(\nu) \sim \nu^4 \sum_{n,\alpha} \int_{\Omega} \frac{P_{\alpha}^{cn}(\boldsymbol{k})}{|\nabla_{\boldsymbol{k}} \varepsilon_{\alpha}(\boldsymbol{k})|} \, \mathrm{d}\Omega \,, \tag{1}$$

where Ω is an isoenergetic surface in $\boldsymbol{k}$-space and $h\nu$ is the energy difference $\varepsilon_{\alpha}(\boldsymbol{k}) - \varepsilon_{cn}$. $P_{\alpha}^{cn}(\boldsymbol{k})$ is the square of the dipole matrix element between the valence band state $\psi_{\alpha\boldsymbol{k}}(\boldsymbol{r})$ and the completely localized state $\varphi_{cn}(\boldsymbol{r} - \boldsymbol{r}_n)$:

$$P_{\alpha}^{cn}(\boldsymbol{k}) = |\langle \varphi_{cn}(\boldsymbol{r} - \boldsymbol{r}_n) | \, \boldsymbol{r} \, | \psi_{\alpha\boldsymbol{k}}(\boldsymbol{r}) \rangle|^2 \,. \tag{2}$$

$\psi_{\alpha\boldsymbol{k}}(\boldsymbol{r})$ may be expanded as a linear combination of atomic orbitals:

$$\psi_{\alpha\boldsymbol{k}}(\boldsymbol{r}) = \frac{1}{\sqrt{N}} \sum_{v,m} c_{vm}^{\alpha}(\boldsymbol{k}) \sum_{l} \mathrm{e}^{i\boldsymbol{k}\cdot\boldsymbol{R}_l} \varphi_{vm}(\boldsymbol{r} - \boldsymbol{r}_m - \boldsymbol{R}_l) \,, \tag{3}$$

where N is the number of unit cells and $c_{vm}^{\alpha}(\boldsymbol{k})$ an expansion coefficient. Substitution of (3) into (2) yields, if all but one-center integrals are neglected,

$$P_{\alpha}^{cn}(\boldsymbol{k}) = \frac{1}{N} \sum_{v,n} |c_{vn}^{\alpha}(\boldsymbol{k})|^2 \, |\langle \varphi_{cn}(\boldsymbol{r}) | \, \boldsymbol{r} \, | \varphi_{vn}(\boldsymbol{r}) \rangle|^2 \,. \tag{4}$$

Combining (1) and (4) and summing over the core states of a unit cell and also over occupied valence states we get

$$I(\nu) \sim \nu^4 \sum_{n,c,v} \sum_{\beta=1}^{3} |M_{vn}^{cn}(x_\beta)|^2 \sum_{\alpha} \int_{\Omega} \frac{|c_{vn}^{\alpha}(\boldsymbol{k})|^2}{|\nabla_{\boldsymbol{k}} \varepsilon_{\alpha}(\boldsymbol{k})|} \, \mathrm{d}\Omega \,. \tag{5}$$

where

$$M_{vn}^{cn}(x_\beta) = \langle \varphi_{cn}(\boldsymbol{r})|\, x_\beta\, |\varphi_{vn}(\boldsymbol{r})\rangle\ ; \qquad x_1 = x\ ,\ x_2 = y\ ,\ x_3 = z\ .$$

The integral in (5) can be replaced by the sum

$$\sum_{\boldsymbol{k}} |c_{vn}^{\alpha}(\boldsymbol{k})|^2\, \delta\big(\varepsilon_\alpha(\boldsymbol{k}) - \varepsilon_{cn} - h\nu\big)\ . \tag{6}$$

With a basis set for the valence band wave functions made up of sulphur 3s and 3p states and nitrogen 2s and 2p states the core states must be given by 1s, 2s, and 2p orbitals on the sulphur and the 1s orbital on the nitrogen atoms. The restriction of the basis to s- and p-states limits the contributions to $I(\nu)$ in (5) to terms containing factors $\langle \mathrm{s}|\, x_\beta\, |p_{x_\beta}\rangle$. Thus, using X-ray spectroscopic notation, $I(\nu)$ can be decomposed in the following manner:

$$I(\nu) = I_{\mathrm{SK}\beta}(\nu) + I_{\mathrm{SL_I}}(\nu) + I_{\mathrm{SL_{II,\ III}}}(\nu) + I_{\mathrm{NK}_\alpha}(\nu)\ , \tag{7}$$

where, for example, $I_{\mathrm{SL_{II,\ III}}}(\nu)$ denotes the emission intensity due to S 3s → 2p transitions. Since the separation of the core level energies is greater that the total bandwidth, each $I_J(\nu)$ covers a distinct frequency interval, and hence may be considered separately. Then, for instance, we may write

$$I(\nu) = I_{\mathrm{SL_{II,\ III}}}(\nu) \sim \nu^4 \sum_{\beta} |M_{\mathrm{SL_{II,\ III}}}(x_\beta)|^2 \sum_{n,\alpha,\boldsymbol{k}} |c_{\mathrm{S3s}}^{\alpha}(\boldsymbol{k})|^2\, \delta(\varepsilon_\alpha(\boldsymbol{k}) - \varepsilon_{\mathrm{S2p}} - h\nu) \tag{8}$$

for those frequencies that correspond to transitions from the valence band to the S 2p state.

We used the Hückel approximation outlined in [8] to calculate the energies $\varepsilon_\alpha(\boldsymbol{k})$ and the coefficients $c_{vn}^{\alpha}(\boldsymbol{k})$. This method has previously been used with good results by Kortela and Manne [24] to determine the σ and π emission spectra of graphite. We have made two modifications of the procedure used in [8]. One was an adjustment of the Wolfsberg-Helmholtz parameter from the value 1.75 to 2 so as to increase the bandwidths in order to achieve closer agreement with photoelectron emission data [25, 26] and with the OPW calculations of Rudge and Grant [10]. A similar change in the Wolfsberg-Helmholtz parameter was also suggested by Kortela and Manne [24]. The second change was the use of the Mikulski et al. [16] crystal structure (as reported by Bright and Soven [11], this second change does not change the band structure significantly).

We use a cartesian coordinate system in which the y-axis is in the direction of the chain axis and the z-axis is perpendicular to the chain plane. This enables us to write for the σ and π emission bands

$$I_J^{\sigma}(\nu) = I_J^{x}(\nu) + I_J^{y}(\nu)\ ,$$
$$I_J^{\pi}(\nu) = I_J^{z}(\nu)\ .$$

The intensity of X-rays polarized parallel and perpendicular to the chain axis is

$$I_J^{\parallel}(\nu) = I_J^{y}(\nu)\ ,$$
$$I_J^{\perp}(\nu) = I_J^{x}(\nu) + I_J^{z}(\nu)\ .$$

The component spectra, $I_J(\nu)$, were calculated for a set of 686 wave vectors which were randomly selected within a uniform mesh in the Brillouin zone. Fig. 1j shows the dependence of the density of states on energy for this sampling of $\boldsymbol{k}$-values. The prominent features of the spectra correspond reasonably closely to the results of the XPS measurements [25, 26]. A value of 0.16 states/(eV-spin-molecule) was calculated for the density of states at the Fermi level, a number which agrees well with the experimental figure of 0.18 states/(eV-spin-molecule) obtained from specific heat measurements [27].

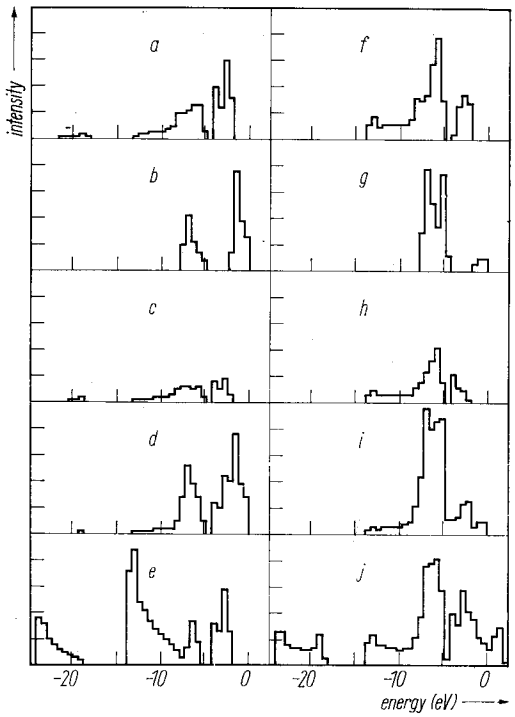

Fig. 1. X-ray emission spectra and the density of electron states for $(SN)_x$. In the case of X-ray spectra the energy plotted is $h\nu - E_F + E_{core}$. The vertical scales in a) to i) are such that only spectra for the same atomic transitions may be compared. a) I^{σ}_{SK}, b) I^{π}_{SK}, c) $I^{\parallel}_{SK}$, d) $I^{\perp}_{SK}$, e) $I_{SL_{II,III}}$, f) I^{σ}_{NK}, g) I^{π}_{NK}, h) $I^{\parallel}_{NK}$, i) $I^{\perp}_{NK}$, j) overall density of states. In the latter curve energy is measured relative to the Fermi energy

The spectra I^{π}, I^{σ}, $I^{\parallel}$, and $I^{\perp}$ for the sulphur K or L_I and $L_{II,III}$ and the nitrogen K emission spectra are presented in Fig. 1, and will be discussed in Section 4.

3. Interband Transitions in the Visible and Near Infrared

Recent reflectivity measurements [19 to 23] prompted us to calculate the interband contribution to the imaginary part $\varepsilon_2(\omega)$ of the dielectric function. The energies and wave functions were calculated in the same manner as we discussed previously. The dielectric function associated with the electric field vector directed along a given direction, $\boldsymbol{e}$, is then given by [28]

$$\varepsilon_2(\omega) = \frac{1}{\pi}\left(\frac{e\hbar}{m\omega}\right)^2 \sum_{a,b} \int |\boldsymbol{e}\cdot\boldsymbol{P}_{ab}(\boldsymbol{k})|^2\, \delta(\varepsilon_a(\boldsymbol{k}) - \varepsilon_b(\boldsymbol{k}) - \hbar\omega)\, \mathrm{d}\boldsymbol{k}\,. \tag{9}$$

In our LCAO formulation the matrix elements take the form

$$\boldsymbol{P}_{ab}(\boldsymbol{k}) = \sum_{i,j} c^{*}_{ai}(\boldsymbol{k})\, c_{bj}(\boldsymbol{k}) \sum_{l} \mathrm{e}^{i\boldsymbol{k}\cdot\boldsymbol{R}_l} \langle \varphi_{ai}(\boldsymbol{r} - \boldsymbol{r}_i + \boldsymbol{R}_l) |\, \nabla_{\boldsymbol{r}}\, | \varphi_{bj}(\boldsymbol{r} - \boldsymbol{r}_j)\rangle\,. \tag{10}$$

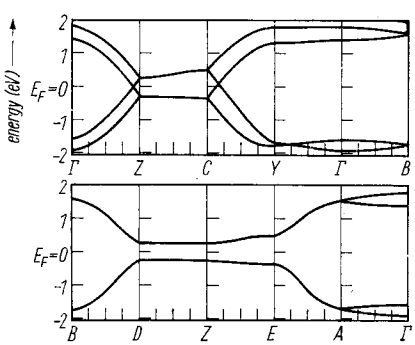

Fig. 2. Energy bands in various symmetry directions. The symmetry points are labelled as in [8]

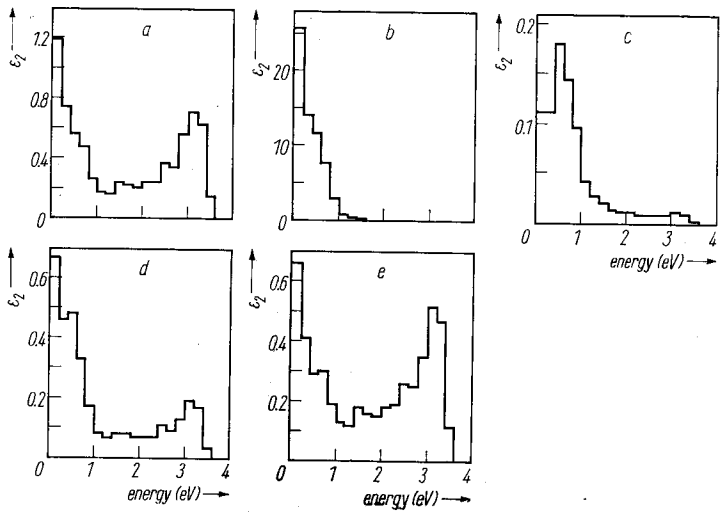

Fig. 3. ε_2 for various incident polarizations: a) $\boldsymbol{E}\|\boldsymbol{x}$, b) $\boldsymbol{E} \| \boldsymbol{y}$, c) $\boldsymbol{E} \| \boldsymbol{z}$, d) $\boldsymbol{E} \| \boldsymbol{c}$ (this corresponds to $\varepsilon_{2\perp f}$ referred to in [21]), e) $\boldsymbol{E} \| \boldsymbol{a}^*$ (this corresponds to ε_{2xx} referred to in [20]). The cartesian axes x, y, z are defined in the text; c is a crystal axis and a^* gives the direction perpendicular to the crystallographic b- and c-axes

Here a, b denote bands above and below the Fermi level, respectively. Since our basis set does not include the sulphur d-orbitals which are expected to influence the higher unoccupied bands, the calculation was restricted to low-frequency transitions between bands straddling the Fermi level (see Fig. 2), i.e. to energies less than 4 eV (for the same reason the comparison made in [23] between theory and experiment above 4 eV does not appear to be meaningful).

The matrix elements in (10) were limited to those between s- and p-orbitals on the same site, p-orbitals on nearest-neighbour S and N atoms on the same chain, and p-orbitals between neighbouring S atoms on the same chain. We also estimated inter-chain matrix elements, but found that we could neglect them since they were an order of magnitude smaller than the matrix elements which we included.

Fig. 3 shows the results for $\varepsilon_2^{\|}$ and $\varepsilon_2^{\perp}$, the dielectric functions for incident radiation polarized parallel and perpendicular to the chain axis (b-axis); a discussion is given in the next section.

4. Discussion

X-ray photoemission spectra essentially only give information about the electron density of states while the X-ray and optical spectra, in principle, give much more detailed information about the nature of the wave functions in the different bands. In the case of the X-ray spectra some of the features would require an analysis of the polarization of the emitted X-rays. There are some features which are independent of polarization and which therefore should be easier to test experimentally. The wave functions in some of the bands are enhanced on either the sulphur or nitrogen atoms and these differences should show up when sulphur and nitrogen X-ray spectra are compared. Furthermore the K and $L_{II,III}$ spectra probe, respectively, the p- and s-like character of the valence band states. In our calculation the conduction band is almost exclusively made up of p-like states and should therefore be weak in the sulphur $L_{II,III}$ spectra if this feature is correct. Similarly, some of the deeper bands are almost completely s-like and should be missing in the K spectra of both sulphur and nitrogen.

If it were possible to make experiments with polarized X-ray emission new features should show up. Since the conduction band is π-like there should be virtually no contribution to the K spectra from this band with polarization in the $(\bar{1}, 0, 2)$ plane (e.g. parallel to the chain axis). This is in contrast to calculations such as that of Kamimura et al. [4, 12] in which there are crossing σ- and π-bands at the Fermi energy. In the latter case a significant intensity I^{σ} or $I^{\|}$ is expected.

The present calculation is carried out within the one-electron approximation. It would be of interest to extend it to include the effect of relaxation around the core hole. One might expect [29] that in the present case many-body effects would be larger than in the nearly free electron metals in which these effects are small.

In addition to being much smaller than $\varepsilon_2^{\|}$ for $\hbar\omega \lessapprox 1$ eV, $\varepsilon_2^{\perp}$ also has some structure at about 3.0 eV. These results contrast with those of Grant et al. [20] who find that $\varepsilon_2^{\perp}$ is much larger than $\varepsilon_2^{\|}$ for frequencies less than 1 eV, but who also obtain a peak at about 0.6 eV. This feature is, they feel, responsible for the peak observed in the reflectivity perpendicular to the chain axis.

The results for $\varepsilon_2^{\|}$ and $\varepsilon_2^{\perp}$ are surprising in view of the overall similarity between the band structures in Fig. 2 and that of [19]. In both cases the proximity of the Fermi energy to band crossings near Z along ΓZ and along CY gives rise to electron and hole pockets, respectively. In the present calculation the pockets are somewhat smaller than in [19] and we do not obtain an open Fermi surface. Except for very small ω we feel this difference should not have a very significant effect on ε_2.

Geserich et al. [21] find as do Grant et al. [20] that the parallel reflectivity $R^{\|}$ can be fitted to a Drude model. In contrast to Grant et al. they demonstrate that $R^{\perp}$ also follows a Drude-like behaviour if the fibrous nature of the $(SN)_x$ crystals are taken into account through an extension of the Maxwell-Garnett theory. From their data, Geserich et al. are able to extract an intrinsic $\varepsilon_2^{\perp}$. In the process of obtaining this intrinsic $\varepsilon_2^{\perp}$ a peak at 0.6 eV evident in the uncorrected result is found to disappear. On the other hand, we have been informed by the authors that the peak in $\varepsilon_2^{\perp}$ observed in [20] will not disappear in a Maxwell-Garnett analysis. Their data is therefore consistent with the large value of $\varepsilon_2^{\perp}$ calculated in [20] and inconsistent with the present results. Because of the short relaxation times in the samples used, the experimental interband transitions are largely swamped by the Drude tail. However, we feel that the results in Fig. 3 are not inconsistent with the results of Geserich et al. [21] which show that in this region the interband contributions to $\varepsilon_2^{\|}$ and $\varepsilon_2^{\perp}$ are much smaller than the Drude terms, and with [22] which show no structure in $\varepsilon_2^{\perp}$.

Since the submission of this paper for publication, several additional articles [30 to 32] describing the band structure of $(SN)_x$ have appeared. Our results for the energy bands and density of states (DOS) agree quite well with the tight-binding calculations of Batra et al. [30] and Ching et al. [31]. The former authors have decomposed their total DOS into contributions from the atomic s- and p-orbitals. From the form of (5) and (6) we see that the X-ray emission intensities, $I(\nu)$, are directly proportional to these partial DOS if the ν^4-dependence is neglected. Thus, for example, adding the spectra in Fig. 1c and 1d gives the density of sulphur 3p states. On making a comparison of Fig. 1 with the results of Batra et al., we observe good agreement in the essential features. Some differences, especially in peak heights, are, no doubt, due to the relatively small sampling of wave vectors in the Brillouin zone in our calculation.

Chelikowsky et al. [32] have also computed s- and p-DOS using a semi-empirical pseudopotential method, and obtained results which are substantially the same as ours and those of Batra et al.

In conclusion, the degree of similarity between the results of our calculation and the more involved ones of [30, 31] certainly recommend the extended Hückel method as a very simple means of determining the tight-binding electronic structure of systems such as $(SN)_x$. Whether or not the agreement between the two methods extends to wave-function-dependent properties is not known since no results of this type (e.g. $\varepsilon_2(\omega)$ as in Fig. 3) are presented in [30, 31].

Acknowledgement

We are grateful to Dr. P. M. Grant for several most helpful conversations and for a correspondence on the subject.

References

[1] R. L. Greene and G. B. Street, in: "Chemistry and Physics of One-Dimensional Metals", Ed. H. J. Keller, Plenum Press, New York 1977; Proc. NATO-ASI, Bolzano (Italy) 1976.
[2] D. E. Parry and J. M. Thomas, J. Phys. C 8, L45 (1975).
[3] V. T. Rajan, and L. M. Falicov, Phys. Rev. B **12**, 1240 (1975).
[4] H. Kamimura, A. J. Grant, F. Levy, A. D. Yoffe, and G. D. Pitt, Solid State Commun. **17**, 49 (1975).
[5] A. Zunger, J. chem. Phys. **63**, 4854 (1975).
[6] M. Kertesz, J. Koller, and A. Azman, Phys. Letters A **55**, 107 (1975).
[7] C. Merkel and J. Ladik, Phys. Letters A **56**, 395 (1976).
[8] W. I. Friesen, A. J. Berlinsky, B. Bergersen, L. Weiler, and T. M. Rice, J. Phys. C 8, 3549 (1975).
[9] M. Schlüter, J. R. Chelikowsky, and M. L. Cohen, Phys. Rev. Letters **35**, 869 (1975); **36**, 452 (1976).
[10] W. E. Rudge and P. M. Grant, Phys. Rev. Letters **35**, 1799 (1975).
[11] A. A. Bright and P. Soven, Solid State Commun. **18**, 317 (1976).
[12] H. Kamimura, A. M. Glazer, A. J. Grant, Y. Natsume, M. Schreiber, and A. D. Yoffe, J. Phys. C **9**, 291 (1976).
[13] D. R. Salahub and R. P. Messmer, Phys. Rev. B **14**, 2592 (1976).
[14] M. Boudeulle, Ph. D. Thesis, Claude Bernard University, Lyon 1974.
[15] M. Boudeulle, Crystal Structure Commun. **4**, 9 (1975).
[16] C. M. Mikulski, P. J. Russo, M. S. Saran, A. G. MacDiarmid, A. F. Garito, and A. J. Heeger, J. Amer. Chem. Soc. **97**, 6358 (1975).
[17] M. J. Cohen, A. G. Garito, A. J. Heeger, A. G. MacDiarmid, C. M. Mikulski, and M. S. Saran, J. Amer. Chem. Soc. **98**, 3844 (1976).
[18] U. Berg, G. Dräger, and O. Brümmer, phys. stat. sol. (b) **74**, 341 (1976).
[19] P. M. Grant, R. L. Greene, and G. B. Street, Phys. Rev. Letters **35**, 1743 (1974).
[20] P. M. Grant, W. E. Rudge, and I. B. Ortenburger, Proc. Conf. Organic Conductors and Semiconductors, Hungarian Academy of Sciences, Siofok 1976, to be published.
[21] H. P. Geserich, W. Möller, G. Scheiber, and L. Pintschovius, phys. stat. sol. (b) **80**, 119 (1977).
[22] A. A. Bright, J. Marshall, A. G. Garito, A. J. Heeger, C. M. Mikulski, and A. G. MacDiarmid, Appl. Phys. Letters **26**, 612 (1975).
[23] J. Bordas, A. J. Grant, H. P. Hughes, A. Jakobson, H. Kamimura, F. A. Levy, K. Nakano, Y. Natsume, and A. D. Yoffe, J. Phys. C **9**, L277 (1976).
[24] E.-K. Kortela and R. Manne, J. Phys. C 7, 1749 (1974).
[25] L. Ley, Phys. Rev. Letters **35**, 1796 (1975).
[26] P. Mengel, P. M. Grant, W. E. Rudge, B. H. Schechtman, and D. W. Rice, Phys. Rev. Letters **35**, 1803 (1975).
[27] R. L. Greene, P. M. Grant, and G. B. Street, Phys. Rev. Letters **34**, 89 (1975).
[28] F. Wooten, Optical Properties of Solids, Academic Press, New York 1972.

[29] V. I. GREBENNIKOV, YU. A. BABANOV, and O. B. SOKOLOV, phys. stat. sol. (b) **79**, 423 (1977).
[30] I. P. BATRA, S. CIRACHI, and W. E. RUDGE, Phys. Rev. B **15**, 5858 (1977).
[31] W. Y. CHING, J. G. HARRISON, and C. C. LIN, Phys. Rev. B **15**, 5975 (1977).
[32] J. R. CHELIKOWSKY, M. SCHLÜTER, and M. L. COHEN, phys. stat. sol. (b) **82**, 357 (1977).

(Received November 21, 1977)